Biochimica et Biophysica Acta 1838 (2014) 372–381

Contents lists available at ScienceDirect

Biochimica et Biophysica Acta

journal homepage: www.elsevier.com/locate/bbamem

Budded baculoviruses as a tool for a homogeneous fluorescence anisotropy-based assay of ligand binding to G protein-coupled receptors: The case of melanocortin 4 receptors

Santa Veiksina, Sergei Kopanchuk *, Ago Rinken

University of Tartu, Institute of Chemistry, Ravila 14a, Tartu, Estonia
Competence Centre on Reproductive Medicine & Biology, Tiigi 61b, Tartu, Estonia

ARTICLE INFO

Article history:
Received 19 July 2013
Received in revised form 19 September 2013
Accepted 24 September 2013
Available online 2 October 2013

Keywords:
Budded baculovirus
Fluorescence anisotropy
Global analysis
G protein-coupled receptor
Melanocortin 4 receptor
Binding kinetics

ABSTRACT

We present here the implementation of budded baculoviruses that display G protein-coupled receptors on their surfaces for the investigation of ligand–receptor interactions using fluorescence anisotropy (FA). Melanocortin 4 (MC_4) receptors and the fluorescent ligand Cy3B-NDP-α-MSH were used as the model system. The real-time monitoring of reactions and the high assay quality allow the application of global data analysis with kinetic mechanistic models that take into account the effect of nonspecific interactions and the depletion of the fluorescent ligand during the reaction. The receptor concentration, affinity and kinetic parameters of fluorescent ligand binding as well as state anisotropies for different fluorescent ligand populations were determined. At low Cy3B-NDP-α-MSH concentrations, a one-site receptor–ligand binding model described the processes, whereas divergence from this model was observed at higher ligand concentrations, which indicated a more complex mechanism of interactions similar to those mechanisms that have been found in experiments with radioactive ligands. The information obtained from our kinetic experiments and the inherent flexibility of FA assays also allowed the estimation of binding parameters for several MC_4 receptor-specific unlabelled compounds. In summary, the FA assay that was developed with budded baculoviruses led the experimental data to a level that would solve complex models of receptor–ligand interactions also for other receptor systems and would become as a valuable tool for the screening of pharmacologically active compounds.

1. Introduction

G protein-coupled receptors (GPCRs), which are members of the largest family of cell surface receptors, are involved in the regulation of a wide range of physiological functions in organisms. GPCRs constitute the primary target group for drug treatment and are of particular interest to the pharmaceutical industry and to fundamental receptor research. The melanocortin receptor family belongs to class A GPCRs and consists of five subtypes of MC receptors. Among them, MC_4 receptors are known as modulators of erectile function and sexual behaviour as well as potential targets for the treatment of depression and anxiety disorders [1]. Because these receptors, like many other pharmaceutically important membrane proteins, are present at low concentrations in native tissues, sensitive methods are required for their detection and characterisation. Radioligand binding was implemented as a method for the detection of receptors in 1965 by Paton and Rang [2], and from henceforth, these so-called "classical" radioactive ligand methods have been widely used for the assessment of receptor–ligand binding as well as for functional assays. Although the radioligand binding method is powerful and still frequently used, it also has several limitations, such as heterogeneity, which requires an additional separation step for the bound and unbound ligand and causes nonequilibrium in the system, as well as safety, waste and cost problems that are associated with radioactive ligands. The availability of novel fluorescent probes with high molecular brightness and stability has led to the development of a set of alternative methods to radioligand binding assays [3]. Among these methods, fluorescence polarisation-, TR–FRET- (time-resolved-Förster/fluorescence resonance energy transfer) and surface plasmon resonance-based assays have found wider recognition and applications [3]. A simple principle, a homogenous system and moderate requirements for equipment would make the polarisation-based fluorescence anisotropy (FA) assay quite attractive for the assessment of GPCR–ligand binding properties. Briefly, this method is based on the phenomenon that population of fluorescent probes emits light with a certain degree of polarisation when excited by plane polarised light; the binding of fluorescent ligands to bigger and more massive receptor proteins changes their freedom of movement that results in a greater extent of polarisation of the emitted fluorescence, which can be measured as a change in the FA signal and followed in

* Corresponding author at: Institute of Chemistry, University of Tartu Ravila 14a, 50411 Tartu, Estonia. Tel.: +372 737 6639; fax: +372 737 5260.
E-mail address: sergei.kopanchuk@ut.ee (S. Kopanchuk).

0005-2736/$ – see front matter © 2013 Elsevier B.V. All rights reserved.
http://dx.doi.org/10.1016/j.bbamem.2013.09.015

real-time without of any separation step requirement. This straightforward approach has been used for the characterisation of the binding properties of numerous proteins [4], which have included only a few GPCRs. Despite its apparent simplicity, there are also several "reefs" that complicate the use of this method for general receptor studies as well as for screening a wide range of receptors from different sources. Changes in fluorescence anisotropy can be detected only if the ratio of bound and free ligands is altered, which means that the concentrations of receptors and ligands have to be comparable. Because most of the GPCRs are normally present at relatively low concentrations in native tissues, it is difficult to achieve measurable changes in the concentration of free ligands. Thus, sufficiently high receptor concentrations in receptor preparations that are used have become a critical requirement for successful FA assay performance. Therefore, receptors from overexpressed or concentrated preparations have been used for this type of experiments. Membranes from overexpressed cells [5–8] or whole cells [9] are primarily used as receptor sources for FA receptor–ligand binding assays. Besides that, cell-free lipoparticle systems have also been proposed as sources of GPCRs for FA assays [10]. Additionally, membrane proteins may be solubilised in the presence of detergent; however, the reconstitution of receptors into liposomes or high-density lipoprotein (HDL) particles could be quite laborious and could also eliminate some important components that may be essential for natural system behaviour. In all these cases, the amount, homogeneity and stability of the receptor preparation seem to limit the broader implications of the assay system for exploratory receptor–ligand binding studies as well as for the high-throughput screening (HTS) of GPCRs. In our previous work we have used membrane preparations from baculovirus infected Sf9 cells (insect cells that were isolated from the pupal ovarian tissue of the fall armyworm *Spodoptera frugiperda*) for the characterisation of the dynamics of ligand binding to MC_4 receptors [11]. However, although good experimental conditions can be achieved, homogenised membranes cannot be considered a homogeneous isotropic assay system—rather a mixture of lipoparticles of different shapes and sizes that range from a few tens of nanometers to more than a micrometre in diameter [24]; additionally, the orientation of receptor proteins within the liposome is a controversial issue with limited control as well. In contrast, it has been shown that receptors that are expressed on the surface of Sf9 cells also bud with baculoviruses and remain on their surface [12]. In this study, we show that a budded baculovirus fraction from Sf9 cells can be successfully used as a preparation for receptors and that this preparation has several advantages over other conventional receptor preparations.

Baculovirus Surface Display (BVSD) technology is based on the ability of baculoviruses to express foreign proteins on both the surface of insect cells and their envelope [13]. Budded baculoviruses are produced during the insect cell infection cycle as nucleocapsids that bud from the insect cell surface. Baculoviruses are rod-shaped viruses (approximately 40–50 nm in diameter and 200–400 nm in length) that are surrounded by a double lipid bilayer envelope, which is derived directly from the host cell surface and carries membrane proteins from the host cell surface. These properties make budded baculoviruses an essentially soluble cell-free system in which membrane proteins, including G protein-coupled receptors, are displayed on the surface of budded baculoviruses in their native conformation and environment. Moreover, BVSD represents more or less a "one size fits all" solution — viruses that are used for the delivery of genetic information into the cells and for the expression of receptors are also used for the exposure of those receptors on their own surfaces. Furthermore, the easy handling (manipulations with baculoviruses could be conducted in Biosafety Level 1 conditions — they are neither hazardous for the environment nor dangerous for humans) and cost-effective large scale production possibilities of the insect cell/baculovirus system would also make this system a highly attractive and useful tool for the assessment of receptor–ligand binding interactions in FA-based assays. In this study, we use the insect cell/baculovirus system to assess melanocortin 4 receptor-ligand binding interactions in an FA-based assay.

2. Materials and methods

2.1. Cell culture and recombinant baculoviruses

Spodoptera frugiperda cells (Sf9) (Invitrogen Life Technologies, Paisley, UK) were maintained as a suspension culture in serum-free insect cell growth medium EX-CELL 420 (Sigma-Aldrich GmbH, Munich, Germany) in Celstir spinner flasks (Wheaton Science Products, USA) (stirring rate 115 rpm) at 27 °C in a nonhumidified environment. The density of the cells was determined with a haemocytometer, and viability was assessed by the exclusion of 0.2% trypan blue (Sigma-Aldrich, USA). Human MC_4 receptors were expressed in recombinant baculoviruses, which were constructed and generated as described previously [11]. Budded baculoviruses expressing NPY_1 receptors (human neuropeptide Y receptor Y1) were used as a control and the same scheme was utilised for NPY_1 receptor recombinant baculovirus generation (with exception that complementary DNA (cDNA) (in pcDNA3.1, obtained from the University of Missouri-Rolla cDNA Resource Center) was subcloned into the BamHI-XbaI site of the pFastBac1 vector). Virus titres were estimated by titration, which was based on viable cell size using a Cell and Particle Counter (Z2™ Series COULTER COUNTER®; Beckman Coulter) [14]. For the production of budded baculoviruses that display MC_4 receptors on their membrane envelope, 500 ml of Sf9 cell suspension at a density of 2×10^6 cells/ml was infected with a high-titer supernatant of baculovirus encoding the MC_4 receptor at a multiplicity of infection MOI = 3 and was grown in a spinner flask for ≈96 h with an agitation of 115 rpm at 27 °C in a nonhumidified environment.

2.2. Budded baculovirus preparation

The supernatant fraction that contained budded baculoviruses was collected after the centrifugation of the Sf9 cell suspension at 1000 ×*g* for 10 min. Following the centrifugation of the collected supernatant at 48,000 ×*g*, the pellet that contained budded baculoviruses was carefully washed with sterile incubation buffer (IB), which contained 20 mM Na-HEPES, 1 mM $CaCl_2$, Complete EDTA-Free Protease Inhibitor Cocktail (according to the manufacturer's description, Roche Applied Science) and 0.1% Pluronic F-127 (Invitrogen), pH 7.4. Then, the baculovirus preparation was concentrated to 20 times the initial cell suspension volume by resuspending the obtained pellet in sterile IB. The preparations were aliquoted and were stored at −90 °C until used for analysis.

2.3. FA measurements in multiwell microplates

The stocks of the fluorescent ligand Cy3B-NDP-α-MSH (GE Healthcare Life Sciences, Sweden) in DMSO were stored at −20 °C and were diluted with assay buffer on the day of the experiment. The concentration of the fluorescent ligand was confirmed by absorbance reading of Cy3B (ε_{558} = 130,000 M^{-1} cm^{-1}). Black 96-well half area, black flat bottom polystyrene NBS microplates (Corning, Product No. 3993) were found to give optimal results for our assays (low background fluorescence and low adsorption of ligands onto the plastic surface) and were used in all experiments.

The FA measurements with budded baculoviruses were performed in IB, which is the simplest buffer solution that is required for ligand binding to the MC_4 receptor. The detergent has been found to be essential for stabilising the signal during anisotropy measurements and has no significant influence on the properties of NDP-α-MSH binding to the MC_4 receptor [11].

The assays were performed in a total volume of 100 μl at 27 °C on a PHERAstar (BMG Labtech, Germany) microplate reader using an optical module with excitation and emission filters of 540 nm (slit 20 nm) and 590 nm (slit 20 nm), respectively. The dual emission detection mode allows the simultaneous recording of intensities that are parallel ($I_{||}$)

and perpendicular ($I_\perp$) to the plane of excitation light. Sensitivities of channels (G factor) were corrected with a gain adjustment of the photomultiplier tubes (PMTs) using erythrosine B as a standard [15].

All experiments were carried out in the kinetic mode at 27 °C (optimal temperature for growing of Sf9 cells). The reactions were started by the addition of the baculovirus preparation to the microplate wells that contained the fluorescent ligand with or without competing ligands, and fluorescence intensities were registered at the appropriate time points. Unless otherwise stated, the baculovirus preparation, which had an MC_4 receptor concentration of approximately 0.5 nM per well (estimated from the results of fluorescent ligand titration experiments with increasing amounts of the baculovirus preparation (described in the Results and discussion)), was used in all experiments.

The ligand-specific effects were measured in the presence (nonspecific binding) or absence (total binding) of an excess of NDP-α-MSH (3 μM, AnaSpec, USA), and specific binding was defined as the difference between these values. In addition, the background fluorescence of the assay, which was caused by membranes, buffers, competing ligands etc., was measured in the absence of the fluorescent ligand and was subsequently subtracted separately from all channels of all the total and nonspecific binding data, resulting in background-corrected values.

The Cy3B-NDP-α-MSH binding saturation to MC_4 receptors was determined by varying the receptor concentration (0–2.1 nM) and keeping the ligand concentration fixed (0.5 nM or 1 nM) or by varying the concentration of Cy3B-NDP-α-MSH (0.1–10 nM) and keeping the receptor concentration constant (0.25 nM or 0.51 nM).

In the case of competitive binding experiments, fixed concentrations of Cy3B-NDP-α-MSH (1 nM) and budded baculoviruses (corresponding to 0.51 nM of MC_4 receptor/well) were incubated with increasing concentrations (0.01 nM–100 μM) of MC_4 receptor agonists (NDP-α-MSH and β-MSH (AnaSpec, USA), α-MSH, Ro27-3225, MT II, HP-228 and H-6268 (Bachem AG, Switzerland), and I-THIQ (kindly provided by Dr. Felikss Mutulis [16])) and antagonists (HS-024 (Tocris Bioscience, UK), SHU9119, JKC-363 and H-2716 (Bachem AG, Switzerland)). The reactions were started by the addition of the baculovirus preparation to the microplate wells and were followed in the kinetic mode as described above. The experiments for all studied MC_4 receptor ligands were performed in duplicates using a 10-point dilution series.

The dissociation kinetics were measured after the preincubation of the budded baculovirus preparation (MC_4 receptor concentration of approximately 0.51 nM) with 1 nM Cy3B-NDP-α-MSH for 6 h. Subsequently, the dissociation was initiated by the addition of 3 μM NDP-α-MSH, 3 μM SHU9119, or 10 mM EDTA (final concentrations), and the reactions were followed in the kinetic mode as described above.

2.4. Data analysis

The background fluorescence (caused by baculoviruses and buffer components in the absence of the fluorescent ligand) was subtracted independently from all intensity channels. Steady-state FA signals at time t after the initiation of the binding reaction were calculated as parameters $r(t)$ from the equation:

$$r(t) = \frac{I(t)_{\parallel} - I(t)_{\perp}}{I(t)_{\parallel} + 2 \cdot I(t)_{\perp}}, \quad (1)$$

where $I(t)_{||}$ and $I(t)_{\perp}$ are the fluorescence emission intensities that were detected from the planes parallel and perpendicular to the beam of the polarisation plane of excitation, respectively. Although fluorescence polarisation and anisotropy describe the same process, FA is usually preferred for quantitative measurements in two or more state systems due to its simpler direct additivity [17]. The FA signal can be defined as the weighted sum of the anisotropy values r_i of the fluorescent ligand in different states i:

$$r(t) = \sum_{i=1}^{n} f(t)_i \cdot r_i, \quad (2)$$

where the weighting parameter $f(t)_i$ describes the fractional proportion of the each fluorescent ligand's state in the corresponding time point, and the sum of fractions is 1. This expression is valid when the total emission intensity (expressed as $I(t)_{\parallel} + 2I(t)_{\perp}$), which reflects the changes of relative quantum yield between fluorescent ligand states, does not change significantly during the binding reaction; otherwise, an enhancement factor correction for each fraction must be implemented [18].

The data fittings were performed in the GraphPad Prism™ 5.04 programme (GraphPad Software, Inc., San Diego, CA, USA) with a built-in Levenberg–Marquart optimisation algorithm or in the Matlab 7.1 programme (MathWorks, Inc., Natick, MA, USA) with the Trust-Region algorithm. The data are presented as the mean ± the standard deviation of at least two independent determinations.

In order to show significance of proper data analysis and challenges connected with its application the more detailed description of developed mathematical solutions for data analysis as well as theoretical justification of calculation process are presented in Theory and Calculations part. Additionally, syntax of used equations for GraphPad Prism™ 5.04 programme is presented in Supplementary data.

3. Theory and calculations

3.1. Budded baculoviruses as an isotropic assay system

One of the conditions that is required for the expression of FA as a function of two orthogonally polarised emission channels (Eq. (1)) is the existence of initial isotropy in the reaction medium. It means that all receptor spatial orientations are evenly distributed and present in the reaction medium. In contrast to soluble receptor/protein studies, the generation of such an isotropic assay system is more challenging when membrane receptors are studied. However, in the case of the BVSD system used, these expectations are primarily fulfilled, which provides new possibilities for obtaining information from the experimental data. Here, for the mathematical description of the real-time kinetics of receptor–ligand binding processes, we implemented models based on ODE (Ordinary Differential Equations) formalism that would make possible to perform detailed calculations of kinetic parameters. It is important to note that ODE solutions imply that the concentration is a continuous quantity. In the case of budded baculoviruses, this idealisation is quite close to the truth due to the small dimensions of baculoviruses and their homogeneous distribution in the medium.

3.2. The global analysis of the FA data

The main asset of the FA method in comparison with radioligand binding assays (which have dominated in studies that test the hypothesis of ligand–receptor interactions) is its inherent applicability for real-time kinetic studies without the disturbance of the processes under investigation. However, the price for this asset is the limited sensitivity of this method for studies of processes where one of the states dominates over another state through the entire reaction. In contrast, it can be considered not as a limitation of the FA method, but as a possibility to a more in-depth study of these processes and in conditions that might be closer to the behaviour of natural systems (often ligand and receptors may have comparable local concentrations). Studies in such conditions demand high quality experimental data and more complex mathematical descriptions of these processes. The information content from single variable experiments is limited and does not allow the non-ambitious description of the underlined complexity of these processes. It has become widely appreciated that the global analysis of data from multiple experiments can significantly increase the information content, which allows a better recovery of parameters and has significantly better model discrimination power. Fluorescence experiments could be conducted and globally analysed using multivariable input parameters (such as initial state concentrations of receptors, ligand and modulators and time), or multivariate output signals with different information

contents (such as FA, fluorescence quantum yield or lifetime) or a mix of both types.

Here, for fine data mining from the experimental results, the exact estimation of nonspecific binding has got different meaning and become increasingly important. In homogenous assay system we have used herewith, the nonspecific binding may have a great impact on estimation of values of total binding as well as the effective concentration of free ligand. Even when the contribution of nonspecific binding to overall FA signal seems to be small it does not automatically mean that nonspecific binding is absent as such and could be neglected; independent experiments for determination of nonspecific binding have to be always carried out. The nonspecific binding of the reporter ligand in the FA assays may have also different nature. For example, the anisotropy of the state of the nonspecific population of the ligand is close to the anisotropy of the state of the free ligand due to retaining the high rotational flexibility of the chromophore's group (although the fluorescent ligand itself could be quite immobile). The reverse situation is also possible when the chromophore alone has high nonspecific binding that leads to the profound loss of its rotational flexibility; thus a small fraction of nonspecific binding may have a great impact on the level of the overall FA signal. The simple subtraction of the nonspecific binding signal from the total binding signal is not the solution as it would lead to the irreversible loss of information about the amount of the ligand that is depleted by nonspecific binding sites. In FA measurements, where main players are fractions of free ligand and specifically bound ligand, this kind misestimation may have a great impact on the results from the data analysis.

The information that could be directly extracted from FA experiments is not sufficient to determine the real parameters that fully characterise nonspecific interactions. However, for estimation of influence of nonspecific binding on the fluorescent ligand concentration available for specific binding we did some assumptions, e.g., nonspecific interactions are very fast and the fraction of the fluorescent ligand that was depleted by nonspecific interactions was defined as an additional binding site with very low affinity. Thus, in the global data fitting procedure, the information content from the specific binding data constrains the parameters of nonspecific binding (and vice versa), which leads to a rigid mechanistic model and improves the fidelity of estimated parameters. In the current study we performed multivariable global analysis based on the simple second-order kinetic model with the existing analytical solution that assumes a maximum of three fluorescent ligand states ($n = 3$) in Eq. (2): free ligand, ligand bound to the receptor and nonspecifically bound ligand. Investigations of more complex models require the implementation of numerical analysis techniques; however, the use of this approach remains beyond the scope of the current paper.

The data from measurements in the presence of a high concentration of the non-labelled ligand that blocks the receptor sites for the binding of the fluorescent ligand were fitted to Eq. (2), which assumes only two possible states of the fluorescent ligand ($n = 2$): free ligand and nonspecifically bound ligand. The nonspecific binding process was much faster in comparison with the kinetics of the ligand binding to the receptor; therefore, it was assumed that time dependence could be ignored and that nonspecific ligand binding could be considered a time invariant process. The fraction of nonspecific ligand binding f^{ns} was modelled according to quadratic Langmuir isotherm taking into the account ligand depletion in the bulk (analogously to Eq. (9)) with the fixed parameter K_d^{ns} (nonspecific binding apparent affinity) and was a function of the known added total concentration of the fluorescent ligand $[L]_T$ and the parameter $[NS]_{stock}$ that was scaled by the volumes of the baculovirus preparation that were added to the well (analogously to Eq. (8)). To avoid ambiguities in connection with the interpretation of the data, the entire data surface of the nonspecific binding data from different experiments (e.g., binding experiments by varying the concentration of the receptors or by varying the concentration of the fluorescent ligand) were globally fitted together with the overall/total binding data. The absolute value of the parameter K_d^{ns} and the number of sites for nonspecific binding $[NS]_{stock}$, do not have real physical meaning when taken alone; however, together these parameters allow the estimation of the concentration of the fluorescent ligand that was depleted by nonspecific binding sites ($[L]^{ns} = f^{ns} \cdot [L]_T$) and defines the concentration of the fluorescent ligand that is available for a specific reaction with receptors ($[L]_{Av}$):

$$[L]_{Av} = [L]_T - [L]^{ns}. \tag{3}$$

The data from the total binding measurements were fitted to Eq. (2), which assumes three possible states of the fluorescent ligand ($n = 3$): free ligand, specifically bound ligand and nonspecifically bound ligand. To obtain good assay performance and obvious changes in the FA signal, the ligand concentration was kept comparable with the concentration of receptors [19], which means that reactions were performed under the conditions of a second order reaction ([L] ≈ [R]), and the ligand depletion has to be taken into the account in the interpretation of the results. Therefore, the association kinetic data were calculated according the general equation for the reversible association of two molecules, which was adopted for these types of experiments [20], where the fraction of the fluorescent ligand bound to the receptor was defined as:

$$f(t)^{sp} = \frac{[RL]}{[L]_T} \cdot \frac{1 - e^{-k_{obs} \cdot t}}{1 + \omega \cdot e^{-k_{obs} \cdot t}}, \tag{4}$$

where [*RL*] is the receptor–ligand complex formed and reflects the amount of the fluorescent ligand that is specifically bound to the receptor:

$$[\mathrm{RL}] = \frac{2k_{\mathrm{on}}[L]_{\mathrm{Av}} \cdot [R]_T}{k_{\mathrm{obs}} + k_{\mathrm{on}}([L]_{\mathrm{Av}} + [R]_T) + k_{\mathrm{off}}}; \tag{5}$$

auxiliary parameter ω in Eq. (4) reflects the deviation of the experimental setup from pseudo first-order kinetics:

$$\omega = \frac{(k_{obs} - k_{on}[L]_{Av} \cdot [R]_T)}{(k_{obs} + k_{on}[L]_{Av} \cdot [R]_T)}; \tag{6}$$

k_{obs} is the observed association rate constant that is mathematically expressed as:

$$k_{obs} = \sqrt{k_{on}^2([L]_{Av} - [R]_T)^2 + k_{off}^2 + 2k_{on}k_{off}([L]_{Av} + [R]_T)}, \tag{7}$$

and k_{on} and k_{off} are the association and dissociation rate constants, respectively. $[R]_T$ is the total receptor concentration in the well, which can be estimated from the results of the fitting procedures. To escape the problem of the identifiability of the parameters, data globalisation was necessary for the kinetic experiments with varying receptor or ligand concentrations. To allow such a possibility, the receptor stock concentration $[R]_{stock}$ was shared, and the $[R]_T$ concentration was scaled to the stock concentration by known dilution factors (the volume of the baculovirus preparation in well V_{BV} per the total reaction volume in well V_{well}):

$$[R]_T = [R]_{stock} \cdot V_{BV}/V_{well}. \tag{8}$$

The dissociation rate constant k_{off} was estimated from independent experiments where the dissociation of the fluorescent ligand was initiated by a high concentration of non-labelled compounds. In the case of a simple one-site binding model, the ligand dissociation from a receptor is a first-order kinetic process and rate constants could be estimated from the single mono-exponential decay fit.

To present the phenomenology of saturation binding behaviour, both types of binding experiments, which vary the concentrations of the fluorescent ligand or receptor, have also been modelled as time-invariant processes (despite the inability to attain equilibrium conditions in the

given ligand–receptor system studied). As in association kinetics experiments, the data from total binding measurements were fitted to Eq. (2), which assumes three possible states of the fluorescent ligand; however, the fraction of specific binding f^{sp} was represented according to the quadratic Langmuir isotherm, which takes into account the bulk depletion of the ligand [21].

$$f^{sp} = \frac{K_d^{sp} + [R]_T + [L]_{Av} - \sqrt{\left(K_d^{sp} + [R]_T + [L]_{Av}\right)^2 - 4 \cdot [R]_T \cdot [L]_{Av}}}{2 \cdot [L]_T}, \quad (9)$$

where K_d^{sp} is the calculated apparent dissociation constant at a certain time point after the initiation of the binding reaction. In the case of true equilibrium conditions, the equilibrium dissociation constant can be estimated by the same procedure.

The data from the competition/displacement binding experiments (varying concentrations of the competitor $[I]_T$ at fixed concentrations of the receptor $[R]_T$ and the fluorescent ligand $[L]_T$) were fitted as previously shown in Eq. (2), which assumes three possible states of the fluorescent ligand, and the fraction of specific binding f^{sp} was represented as [22,23]:

$$f^{sp} = \frac{2 \cdot \sqrt{(a^2 - 3b)} \cos(\theta/3) - a}{3 \cdot K_d^{sp} + 2 \cdot \sqrt{(a^2 - 3b)} \cos(\theta/3) - a}, \quad (10)$$

where a, b, c and θ are auxiliary parameters that are expressed as:

$$a = K_d^{sp} + K_i^{app} + [L]_{Av} + [I]_T - [R]_T, \quad (11)$$

$$b = K_d^{sp} \cdot \left([L]_{Av} - [R]_T\right) + K_i^{app} \cdot \left([I]_T - [R]_T\right) + K_d^{sp} K_i^{app}, \quad (12)$$

$$c = -K_d^{sp} K_i^{app} \cdot [R]_T, \quad (13)$$

$$\theta = \arccos \frac{-2a^3 + 9ab - 27c}{2 \cdot \sqrt{(a^2 - 3b)^3}}, \quad (14)$$

and K_i^{app} is the competitor's inhibitory dissociation constant.

4. Results and discussion

4.1. The implementation of budded baculoviruses as a source of receptors for FA signal measurements

The budded baculoviruses that were used in this report were collected 96 h after the infection of Sf9 cells with MOI = 3. This procedure has been found to be best choice after the optimisation of experiments where the infection time varied from 48 to 120 h and the MOI varied from 3 to 30 (data not shown). However, it is necessary to emphasise that these conditions were only optimal for MC_4 receptors. In experiments where the BVSD system has been used for the production of other GPCRs, e.g., NPY_1 and $5HT_{1A}$ receptors, the optimal infection times and MOI values were different (data not shown). The collected MC_4 receptor baculoviruses were concentrated by simple centrifugation at 48,000 ×g and were resuspended into the incubation buffer. Obtained baculovirus preparation demonstrated MC_4R specific ligand binding with good FA assay performance and stability (Fig. 1). The intensity of the autofluorescence and light-scattering from the baculovirus preparation was more than five times lower than that observed with the membrane preparations of Sf9 cells that expressed MC_4 receptors [11] and was comparable with the fluorescence intensity of 0.1 nM Cy3B-NDP-α-MSH. Because this low fluorescence level had no significant influence on the quality of the FA signal that was determined, we have used the simplest way to separate the cell and virus fractions to obtain the budded baculovirus preparation and to avoid additional purification and fractionation steps that have been proposed previously by other authors [12,25]. Furthermore, because the baculovirus preparation can be easily concentrated, our experience has shown that even a 100 nM receptor stock concentration could be without difficulty achieved.

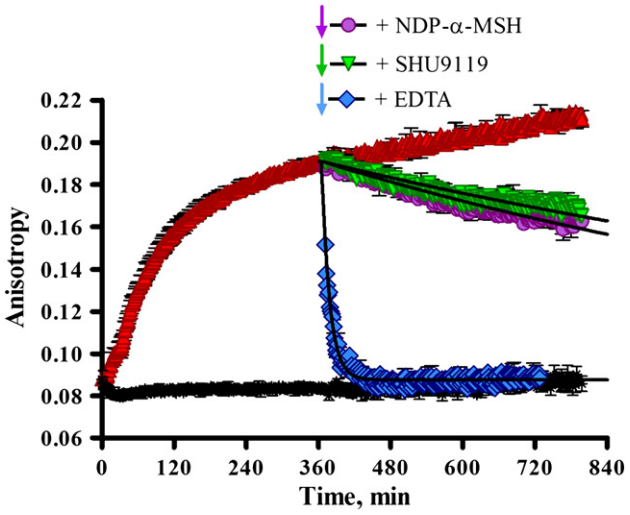

Fig. 1. Time course of anisotropy changes that were caused by the binding of Cy3B-NDP-α-MSH to MC_4 receptors in the budded baculovirus preparation and the subsequent dissociation of formed receptor–ligand complexes. Reactions of Cy3B-NDP-α-MSH (1 nM) binding to the MC_4 receptors (0.51 nM) in the presence (∗) or absence (Δ) of 3 μM non-labelled NDP-α-MSH were initiated by the addition of the budded baculovirus preparation to the reaction mixtures. At the indicated time points, fluorescence intensities were measured, the background was corrected, and anisotropy values were calculated according to Eq. (1). At the 360 min time point, the dissociation reactions were initiated (indicated by arrows) by the addition of 3 μM NDP-α-MSH (○), 3 μM SHU9119 (▽), 5 mM EDTA (◇) or a buffer solution (Δ), and the reactions were further followed in duplicates for at least the next 6 h. The dissociation rate constants k_{off} were estimated from single mono-exponential decay fits with shared EDTA and the initiated dissociation of ligands trace amplitudes of anisotropy changes and lines represent fits of the data. The data of the representative experiments from three independent experiments that were performed are shown as the mean ± the standard deviation.

The pharmacological properties (discussed later) of MC_4 receptors in the budded baculovirus preparation was not affected by freezing and thawing, and the receptor concentration in the preparation remained constant for at least 6 months during the storage of the preparation at −90 °C (data not shown).

An essential advantage of baculoviruses over membrane preparations is the stability of baculoviruses in solutions as well as the stability of the measured FA signal. After the addition of baculoviruses to the reaction medium, the signal remained stable for at least 12 h, which is necessary for assays when slowly binding ligands are studied or when large massifs of samples are being screened at the same time. In the case of membrane preparations from the same cell system, the signal started to decrease after only 3 h of incubation [11].

It should be mentioned that although retrovirus generated virus-like particles (VLPs) with chemokine receptors CXCR4 on their surfaces have been used in FA assays [10], however, our past experience has found that the medium/high scale production and purification of Murine Moloney Leukemia Virus VLPs with MC_4 receptors can be quite challenging in terms of costs and the stability of the receptor preparation over time (not shown).

4.2. The kinetics of MC_4 receptor and Cy3B-NDP-α-MSH interaction

Herewith we have used only a multivariable global analysis (instead of multivariate output signal analysis or mix of both types) primarily because the chromophore emission of the fluorescent ligand Cy3B-NDP-α-MSH did not significantly change in the presence of the MC_4R baculovirus preparation in the reaction mixture (the difference below 5% between the background corrected total fluorescence emission of

free and receptor–bound ligand). This ruled out the possibility that the observed time-dependent increase of the FA signal (Fig. 1, Δ) is caused by some complex photophysical processes (changes in fluorescence quantum yield or fluorescence lifetime, or due to homo-FRET) and not as a result of a specific receptor–ligand binding event. The specificity of the binding event was verified in the presence of 3 μM NDP-α-MSH, which blocked MC_4 receptors for binding with the fluorescent ligand (Fig. 1, ✳); no significant time-dependent changes in fluorescence anisotropy values were observed. Moreover, no specific Cy3B-NDP-α-MSH binding was observed in control experiment performed in similar conditions but with baculoviruses expressing NPY_1 receptors (Supplementary Fig. S1); it confirms that budded baculoviruses by itself do not contain any additional binding places for Cy3B-NDP-α-MSH.

At least a partial reversibility of Cy3B-NDP-α-MSH binding to the MC_4 receptor was demonstrated by a time-dependent decrease in the signal after the addition of an excess of competitive melanocortin ligands to the reaction medium after a 6 h preincubation for the complex formation. Due to the extremely slow dissociation process, it was practically impossible to determine its final level. However, it was assumed that the signal amplitudes of dissociation that are caused by a competitive ligand would be the same as in the case when the dissociation was initiated by the addition of EDTA (the validity of this assumption is discussed later). Addition of 10 mM EDTA caused a rapid decrease in the FA signal to a nonspecific level (Fig. 1, ◇), which is connected with the removal of Ca^{2+} from the reaction medium by EDTA and subsequent release of Cy3B-NDP-α-MSH from the complex with MC_4 receptor in the absence of the bivalent cation [11,26,27]. Calculated $k_{off,EDTA}$ for this process was $0.054 \pm 0.001\ min^{-1}$. Instead, when dissociation was initiated by an excess of agonist (3 μM NDP-α-MSH, Fig. 1, ○), the process was slow with a calculated $k_{off,NDP\text{-}\alpha\text{-}MSH}$ of $(8.8 \pm 2.0) \times 10^{-4}\ min^{-1}$ ($n = 3$). In the case of dissociation that was initiated by an antagonist (3 μM SHU9119, Fig. 1, ▽), the calculated off-rate constant was $k_{off,SHU9119} = (6.8 \pm 1.5) \times 10^{-4}\ min^{-1}$ ($n = 2$), which indicated no significant difference in off-rates and no dependence on the nature of the competitive ligand used.

The flexibility and signal quality of the new assay system used allowed us to use global analysis to describe the kinetics of the association process. In our previous studies using the Sf9 cell membrane preparation that expresses MC_4 receptors [11], the accuracy of the assay format allowed us to extract only phenomenological descriptors of association kinetics (the observed rate constant (k_{obs}), observed overall anisotropy and parameter ω that we used to describe the deviation of the experimental setup from pseudo-first-order kinetics). Here, we applied a more exact analytical expression to the orthogonal data sets for the simultaneous fit of two data surfaces (overall/total and nonspecific binding signals) as a function of both time and the concentration of receptors, at a fixed (0.5 nM) concentration of the fluorescent ligand (Fig. 2). Generally, the input concentrations of fluorescent ligands in FA assays are precisely known, whereas membrane receptor concentrations often remain poorly defined. To make the practically possible estimation of receptor concentrations, a new parameter $[R]_{stock}$ (receptor concentration in stock solution) was introduced. Accordingly, the input concentration of receptors in assays could be defined as the receptor concentration in the stock solution, which was scaled by known dilutions (Eq. (8)). Such an approach removed the problem of the identifiability of this parameter, and the estimated receptor concentration in the stock was found to be 6.9 ± 0.3 nM. The global analysis of the current kinetic experiments allowed the determination of anisotropies for different fluorescent ligand states as well: anisotropy of the free ligand $r_{free} = 0.074 \pm 0.003$; anisotropy for the nonspecifically bound ligand $r_{ns} = 0.114 \pm 0.003$; and anisotropy for the ligand that was specifically bound to the receptor $r_{bound} = 0.292 \pm 0.009$. Here, it is interesting to mention that we have also determined limited anisotropy for Cy3B-NDP-α-MSH by using two independent methods: steady state anisotropy from the Perrin–Weber plot and TCSPC (Time Correlated Single Photon Counting) anisotropy decay; both methods gave a limited anisotropy value of 0.354 (data not shown). The anisotropy value of the bound ligand that was calculated from our receptor binding experiments is quite close to that limit; nevertheless, the difference may be explained by the contribution of the so-called "propeller effect" of the bound ligand and/or ligand, in which the binding pocket has retained slight flexibility ("local" motion). However, the experimentally observed values of the overall signal at saturating receptor concentrations (Fig. 2) were also lower than the calculated value of r_{bound}, probably caused by nonspecific interactions that decreased maximally possible anisotropy value of overall signal. It could also be speculated that the relatively fast "global" motion of baculoviruses that express receptors also decreases the overall anisotropy signal. However, the Debye rotational time for a spherical protein with a molecular mass of approximately 40 kDa (it is the pure protein without membrane) is over 50 ns, and the measured fluorescence lifetime of our molecule is 2.72 ± 0.02 ns, the calculated theoretical overall anisotropy values of the whole complex is substantially greater than 0.3, and cannot affect measurable here parameters. Thus, the "global" motion of membrane receptors, which are expressed in baculoviruses as well as in membrane preparations, the rotation is so slow that the "size does not matter" in both receptor preparation cases if we use fluorophores with a relatively fast lifetime. Equipment bias, which would also possibly decrease the observed anisotropy signal, was ruled out by the fact that the value of limiting anisotropy (from Perrin–Weber plot) was determined on the same equipment with the same calibrations.

The global analysis of the data from association kinetics (Fig. 2) also allowed the determination of the on-rate kinetic parameters for the second-order binding reaction; k_{on} was found to be $(1.44 \pm 0.11) \times 10^7\ M^{-1}\ min^{-1}$. During this fitting procedure, k_{off} was constrained to the value that was determined from the dissociation experiments using 3 μM NDP-α-MSH and that assumed monoexponential decay for all receptor populations (described above). The receptor–ligand dissociation constant K_d was calculated from kinetic parameters, where $K_d = k_{off}/k_{on} = 0.06$ nM. The removal of this constraint for k_{off} significantly improved the fit of the parameters ($P < 0.0001$) and revealed another k_{off} value ($(3.1 \pm 0.4) \times 10^{-3}\ min^{-1}$) as well as slightly influenced k_{on} ($(1.0 \pm 0.2) \times 10^7\ M^{-1}\ min^{-1}$) and $[R]_{stock}$ (7.4 ± 0.4 nM) parameters. A similar off-rate constant for Cy3B-NDP-α-MSH dissociation can also be obtained from the direct experiment that has been described above; however, in this case there was a non-dissociating fraction, which composed $57 \pm 5\%$ of the entire observed binding signal. Unfortunately, because the dissociation process was extremely slow, and it was practically impossible to follow this process longer, the low discriminative power of the current data analysis prevents us from making clear decisions about the exact final level of the dissociation reaction and the mechanism of reaction. Furthermore, the existence of binding sites with different affinities became more evident when association binding experiments were performed with a higher concentration of Cy3B-NDP-α-MSH (1 nM) and varying receptor concentrations; it was already impossible to find a satisfactory one-site binding global fit for those data. These results suggest a more complex mechanism for receptor–ligand interactions. However, more experiments that implement numerical modelling would be required in the future to understand this aspect.

4.3. Phenomenology of Cy3B-NDP-α-MSH binding to MC_4 receptors

Implementation of FA method allows overcome limiting experimental conditions of typical radioligand binding assays requiring large excess of used radioligand concentration over receptor concentration (pseudo-first-order reaction conditions). Thus, we have performed two types of receptor–ligand titration experiments: by keeping fluorescent ligand concentrations constant (1 or 0.5 nM) and varying the concentration of receptors, or by keeping the amount of receptors constant and varying the concentration of Cy3B-NDP-α-MSH. Fig. 3 presents time snapshots of binding reactions after 3 h of incubation. Although it is clear from the presented kinetic experiments that the equilibrium conditions of

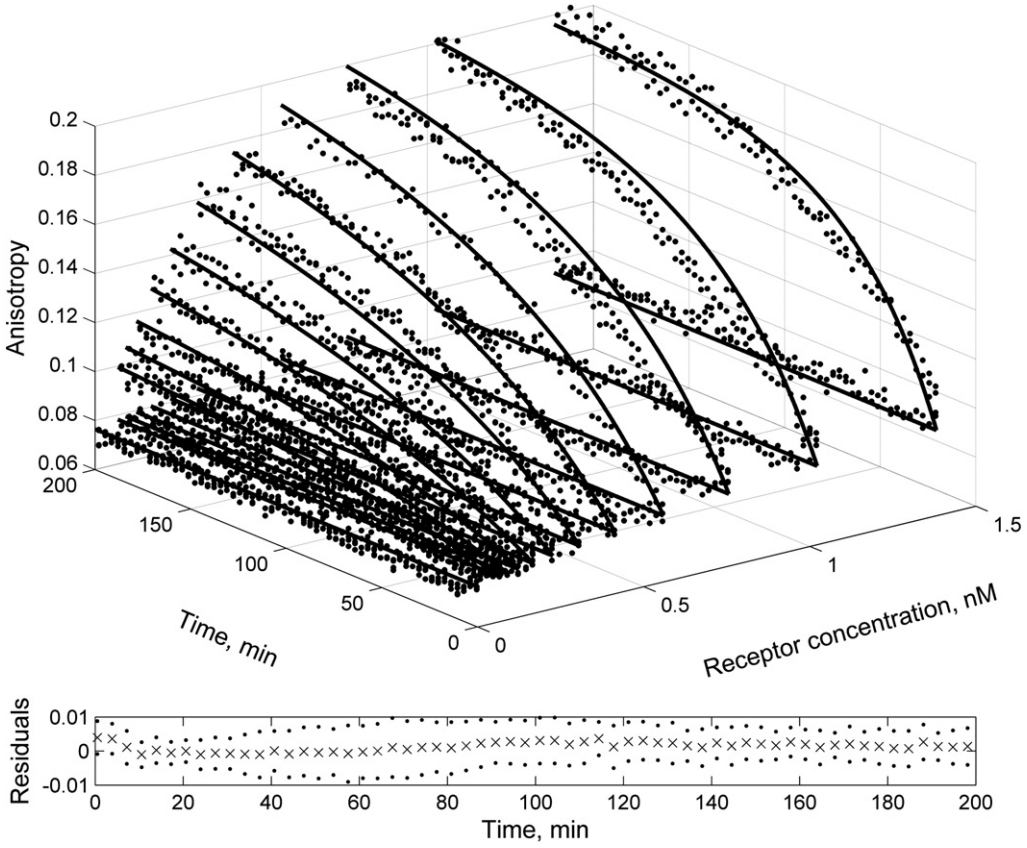

Fig. 2. Association kinetics of 0.5 nM Cy3B-NDP-α-MSH binding to different concentrations of MC_4 receptors in the budded baculovirus preparation. Reactions of Cy3B-NDP-α-MSH binding to the MC_4 receptors were initiated by the addition of different amounts of the budded baculovirus preparation to the reaction mixtures (upper panel). At the indicated time points, fluorescence intensities were measured, the background was corrected, and anisotropy values were calculated according to Eq. (1). Two experimental data surfaces, one in the presence and one in the absence of 3 μM non-labelled NDP-α-MSH, were globally fitted for retrieving a consistent solution according to Eqs. (2)–(**8**). The lines represent the results of the non-linear optimisation procedure. The final concentrations of the MC_4 receptor binding sites in the wells were posteriorly calculated after global fitting and were presented on the receptor concentration axis (1.26, 0.93, 0.69, 0.51, 0.38, 0.28, 0.21, 0.153, 0.113, 0.083, 0.062 and 0 nM). Each data point from the representative experiments of the two independent experiments that were performed in duplicate is shown. The distribution of residuals between the experimental data and the global fit is presented on the lower panel as the mean of all time courses (×) ± the standard deviation (dashed lines).

receptor–ligand binding are not reached at that time, we applied a set of equations derived for equilibrium conditions (Eqs. (2)–(3), (8)–(9)) to demonstrate the phenomenology of the observed behavioural differences between these two types of experiments.

Increase of receptor concentration at fixed ligand concentrations led to "hyperbole-like" increase of FA values (Fig. 3A) and, as it was expected, higher ligand concentrations required higher concentration of receptors to achieve saturation of observed FA signal. Global fitting of the data from both binding isotherms to equations (Eqs. (2)–(3), (8)–(9)), gave the apparent K_d value 0.07 ± 0.02 nM and estimated $[R]_{stock}$ concentration 9.7 ± 0.5 nM. These estimates are close to the corresponding values obtained from kinetic experiments. However, a dramatically different situation appeared when fixed receptor concentrations were titrated with different ligand concentrations (Fig. 3B). It was expected that higher receptor concentrations would result in higher FA values, but it was not expected that the observable drop in the FA signal with an increase in the concentration of the fluorescent ligand would be so small. According to previously estimated parameters, we estimated that at a 10 nM concentration of Cy3B-NDP-α-MSH, the fraction of free ligand would dominate and that the observable FA signal would be low (simulations shown as dashed lines on Fig. 3B). However, the global fitting of the experimental data to the equations (Eqs. (2)–(3), (8)–(9)) gave the apparent K_d value of 4.0 ± 0.4 nM, and the calculated concentration of receptors in stock $[R]_{stock}$ was 36 ± 4 nM. Accordingly, it is proposed that higher Cy3B-NDP-α-MSH concentrations make it possible to reveal the appearance of additional low affinity MC_4 receptor binding sites that are "invisible" at lower fluorescent ligand concentrations. However, the data available do not allow the clearly discrimination of these different binding sites; besides, in this study, for the data analysis we have used analytical mathematical solutions that have limitations in their applications for the analysis of complex binding models.

Attempts to find a unified solution by the simultaneous global fitting of the data from both types of receptor–ligand binding experiments did not give satisfactory results. One can argue that this observation is due to the inability to reach equilibrium that is an essential condition for the application of the equations used. However, this argument is not the case; as shown in Fig. 4, the divergence between the expected kinetic behaviour (dashed lines) and the signal detected (plotted data points) grows and in time becomes more and more evident at higher ligand concentrations. In addition, the increase in the detected signal cannot either be addressed to the possibly growing impact of nonspecific interactions because the nonspecific binding signal remains constant in all studied fluorescent ligand concentrations (the limiting case of the nonspecific signal that was obtained by the largest Cy3B-NDP-α-MSH concentration used (10 nM) is depicted in Fig. 4 as black (**1**)).

Taken all the presented data together, we have shown that at low concentrations of Cy3B-NDP-α-MSH the interactions between the fluorescent ligand and the MC_4 receptor could be described as a simple one-site binding process, whereas at higher concentrations of Cy3B-NDP-α-MSH the complexity of the receptor–ligand interaction becomes more evident. It is obvious that the currently used fluorescent analogue of NDP-α-MSH and the previously used radiolabelled ^{125}I-NDP-α-MSH [27,28] should be considered chemically different molecules; we cannot

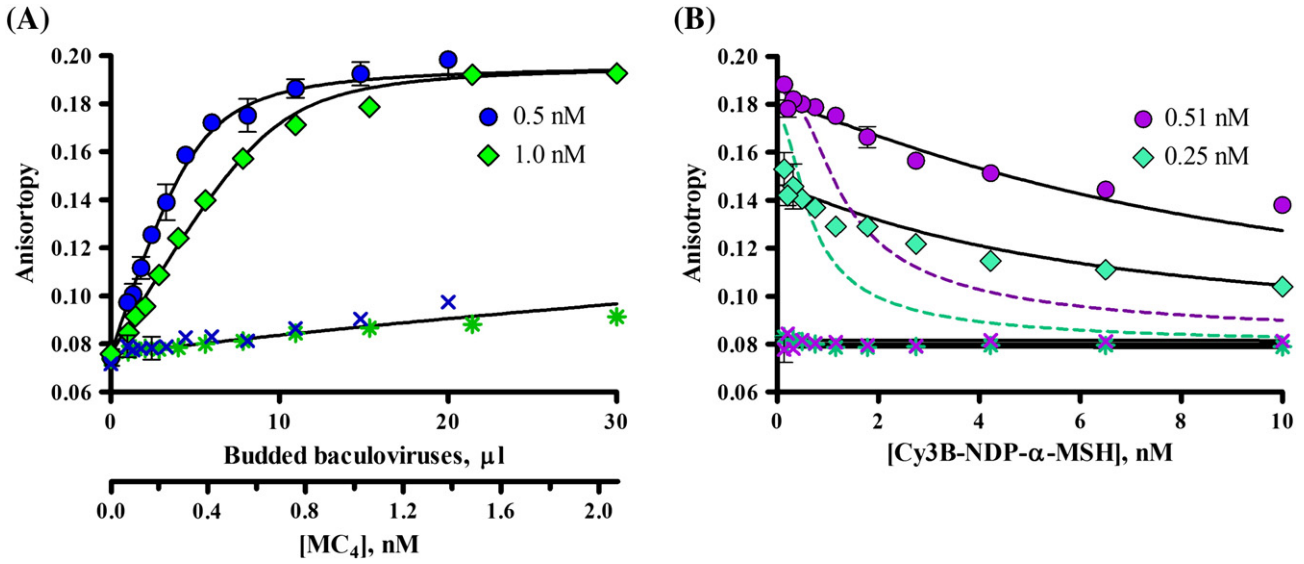

Fig. 3. Time snapshots of Cy3B-NDP-α-MSH binding curves to MC_4 receptors by varying receptor concentration (A) and by varying concentration of Cy3B-NDP-α-MSH (B). A. Fixed concentrations of Cy3B-NDP-α-MSH — 0.5 nM (○, ×) and 1 nM (◇, ✳) were incubated with increasing amounts of the MC_4 receptor budded baculovirus preparation (0–30 µl/well, depicted on the upper x-axis) in the absence (○, ◇) or presence (×, ✳) of 3 µM non-labelled NDP-α-MSH. After a 3-h incubation period, fluorescence intensities were measured, the background was corrected, and anisotropy values were calculated according to Eq. (1). The lines correspond to the global fit of the binding data to the set of equations (Eqs. (2)–(3), (8)–(9)). Corresponding MC_4 receptor binding site concentrations that are depicted on the lower x-axis were calculated posteriorly from this data fitting. B. Fixed concentrations of MC_4 receptors in budded baculovirus preparation – 0.51 nM (○, ×) and 0.25 nM (◇, ✳) – were incubated with increasing concentrations of Cy3B-NDP-α-MSH (0.1–10 nM) in the absence (○, ◇) or presence (×, ✳) of 3 µM non-labelled NDP-α-MSH. After a 3-h incubation period, fluorescence intensities were measured, background corrected, and anisotropy values were calculated according to Eq. (1). The solid lines correspond to the global fit of the binding data to the set of equations (Eqs. (2)–(3), (8)–(9)). The dotted lines represent the projections of the one-site binding model with parameters that were determined from type (A) saturation binding experiments where ligand binding to the MC_4 receptors was determined by fixed concentrations of Cy3B-NDP-α-MSH to increasing concentrations of MC_4 receptors. The data of the representative experiments from two independent experiments performed in duplicates are shown as the mean ± the standard deviation.

directly extrapolate the previously obtained conceptions and models based on the results of the current study. In spite of that, these two ligands have many similarities in their pattern of interaction with the MC_4 receptor, and in the present work we also observed the emergence of additional lower affinity receptor–ligand interaction sites with slow association kinetics. Thus, the current results do not contradict our previous interpretation of this phenomenon, which was a modelled assuming existence of two tandemly arranged MC_4 receptor binding sites on a dimeric receptor unit [28].

The table of obtained parameters with corresponding comments are summarized in the Table S1 in Supplementary data part of the paper.

4.4. Displacement of Cy3B-NDP-α-MSH binding from MC_4 receptors

Because of the quality of the budded baculovirus-FA assay system and the increased information content of the kinetic experiments, we were able to receive well-defined parameters to describe ligand–

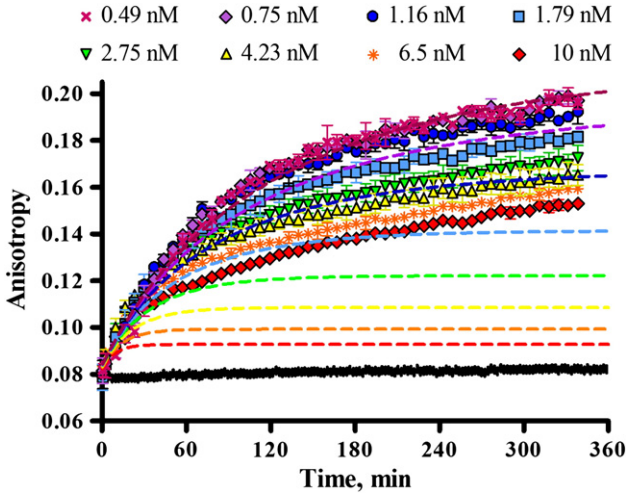

Fig. 4. Association kinetics of Cy3B-NDP-α-MSH to the MC_4 receptors in the budded baculovirus preparation. The reactions of Cy3B-NDP-α-MSH binding (concentrations indicated in figure) to the MC_4 receptors (0.51 nM) were initiated by the addition of the budded baculovirus preparation to the reaction mixtures. The dashed lines represent the theoretical behaviour of time traces, when a one-site binding model with parameters extracted from the kinetic global fit of Cy3B-NDP-α-MSH binding (0.5 nM) to different amounts of receptors was used. An increase in the concentration of Cy3B-NDP-α-MSH caused a clearly observable deviation from the expected one-site binding model behaviour. A time trace of 10 nM Cy3B-NDP-α-MSH binding in the presence of 3 µM NDP-α-MSH is also shown to indicate nonspecific binding (ı). The data of the representative experiment that was performed in duplicates are shown as the mean ± the standard deviation.

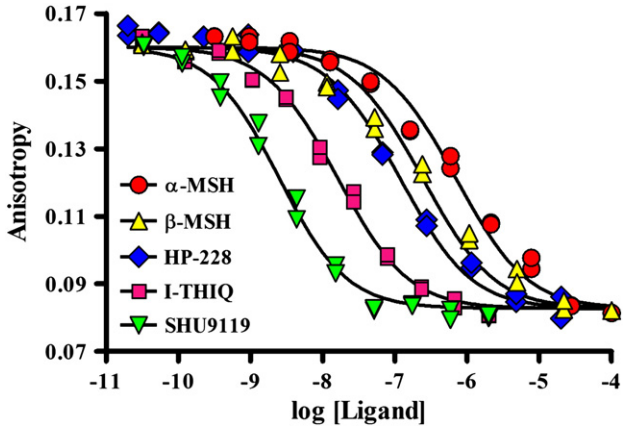

Fig. 5. The influence of different MC_4 receptor ligands on the binding of Cy3B-NDP-α-MSH to the MC_4 receptor in budded baculoviruses. The baculovirus preparation (0.51 nM MC_4 receptors/well) was added to the reaction mixtures containing 1 nM Cy3B-NDP-α-MSH and the indicated concentration of competitors. After 3 h of incubation, fluorescence intensities were measured, background corrected, and anisotropy values were calculated according to Eq. (1). The lines represent the fitting of the data to the set of equations (Eqs. (**2**)–(**3**), (**8**), (**10**)–(**14**)). The data presented are from representative competition binding experiments from at least two independent experiments that were performed in duplicates after 3 h of incubation period.

Table 1
Apparent binding affinities of ligands to MC_4 receptors in budded baculoviruses that were obtained in competition with 1 nM Cy3B-NDP-α-MSH.

Agonists			Antagonists		
	K_i^{app} [a]	n		K_i^{app} [a]	n
MT II	0.3 ± 0.2	2	SHU9119	0.27 ± 0.12	2
NDP-α-MSH	0.47 ± 0.18	4	JKC-363	0.51 ± 0.18	2
H-6268	0.73 ± 0.17	2	HS-024	1.8 ± 0.6	3
I-THIQ	1.4 ± 0.3	3	H-2716	35 ± 16	2
HP-228	8 ± 3	2			
β-MSH	22.5 ± 1.6	3			
α-MSH	42 ± 9	3			
Ro27-3225	78 ± 25	2			

[a] After a 3-h incubation, apparent binding affinities were calculated by fitting the data from competition experiments to the set of equations (Eqs. (2)–(3), (8), (10)–(14)) and were expressed as the ligands' inhibitory dissociation constant K_i^{app}. The values are given in nM ± the standard deviations of n experiments carried out in duplicates.

receptor interactions in conditions where the complexity of the system behaviour still does not have a dominant character. The obtained parameters of Cy3B-NDP-α-MSH and MC_4 receptor interactions were used to analyse the data for competition experiments. For the pharmacological characterisation of MC_4 receptors in budded baculoviruses, eight different MC-specific agonists and four antagonists were compared with their ability to compete with Cy3B-NDP-α-MSH. All studied ligands caused a concentration-dependent decrease in the FA signal of 1 nM Cy3B-NDP-α-MSH, which had their half maximal effect in the submicromolar range (Fig. 5). The receptor concentration used was 0.51 nM, and it was estimated that 26% of ligand was depleted by nonspecific binding at these conditions. The fitting of the experimental data to the set of equations (Eqs. (2)–(3), (8), (10)–(14)) revealed the apparent K_i^{app} values (listed in Table 1), which are in agreement with the apparent affinities that were determined using other methods [1,29]. Because the system has not reached equilibrium, these values can be considered only as apparent inhibition constants. We have shown that even incubations longer than 12 h with Cy3B-NDP-α-MSH do not reach the binding equilibrium with MC_4 receptors under second-order reaction conditions (Fig. 1). Taking into account the slow dissociation kinetics of NDP-α-MSH and the a priori unknown kinetic properties of the competitive ligand, we have a transient system, where even apparent potencies change in time [11]. Here, we have used the kinetic mode for monitoring the reaction, which allows the measurement of the data from the most suitable time point. We have selected 3 h from the beginning of the reaction because this time has previously been widely used for the characterisation of ligand binding properties to MC receptors (see references in [30]).

As discussed previously, in the FA method we are able to use a receptor concentration that is comparable with the concentration of the fluorescent ligand. In these conditions, ligands compete primarily for the high affinity sites. This observation may explain why a relatively homogenous competition pattern has been observed in the majority of displacement experiments (instead of the heterogeneous displacement curves that have been obtained in radioligand competition experiments where the radioligand/receptor concentration ratios was much higher than 10) [27].

5. Conclusions

Despite the availability of numerous conceptually different approaches for the characterisation of ligand–receptor interactions, there remains a great requirement for complementary methods that are suitable for kinetic studies, especially for the characterisation of membrane protein systems. The FA method inherently fits well for this purpose. In comparison to classical radioligand binding assays, there are no additional perturbing separation steps in the FA method. Furthermore, in contrast with well-established surface-sensitive techniques, such as SPR, that are also used for the real-time monitoring of ligand–receptor interactions, general complexities concerning the mass transfer limitation do not greatly influence FA assays. Moreover, label-free methods often have inherent limitations with sensitivity, whereas the majority of new highly sensitive fluorescence techniques require additional modifications in the structure of membrane receptor proteins; promising so-called "single-molecule techniques" remain still in the early stages of their development.

The current study presents a general framework for the characterisation of ligand–receptor interactions by the FA method with the implementation of BVSD technology. FA based ligand–receptor binding assays on baculoviruses would be beneficial in terms of the homogeneity of the receptor preparation, the receptor concentration and a better signal to noise ratio as well as the stability of the preparation in long-term experiments. We also set up a new strategy for the analysis of the FA kinetic data with analytical expressions; this new strategy partially compensates for some limitations that appear when the FA method is applied to membrane receptor studies. In particular, we consider the effect of nonspecific interactions on the concentration of the free fluorescent ligand and the difficulties that are related to the inability to know the input concentration of membrane receptors a priori.

Combining the BVSD platform with stopped-flow and microfluidic systems with fluorescence correlation spectroscopy (FCS) or total internal reflection fluorescence (TIRF) read-outs in the future would lead to efficient assays that would allow even more detailed studies of ligand-binding kinetics. Because our parallel project implements global analysis with numerical integrations, we intend to present an extension of the current work for the screening of the kinetic parameters of drug candidates from competitive FA assays [31]. We hope this project would be an important tool for both academic and industrial life science research.

Acknowledgements

The work was funded by the Estonian Science Foundation (8314), the Estonian Ministry of Education and Science (SF0180032s12) and the European Union through the European Regional Development Fund (TK114, 30020). We thank Indrek Viil and Kerli Martin for preparation of budded baculoviruses expressing NPY_1 receptors.

Appendix A. Supplementary data

Supplementary data to this article can be found online at http://dx.doi.org/10.1016/j.bbamem.2013.09.015.

References

[1] J.E.S. Wikberg, F. Mutulis, Targeting melanocortin receptors: an approach to treat weight disorders and sexual dysfunction, Nat. Rev. Drug Discov. 7 (2008) 307–323.
[2] W.D. Paton, H.P. Rang, The uptake of atropine and related drugs by intestinal smooth muscle of the guinea-pig in relation to acetylcholine receptors, Proc. R. Soc. Lond. [Biol.] 163 (1965) 1–44.
[3] L. Chen, L. Jin, N. Zhou, An update of novel screening methods for GPCR in drug discovery, Expert Opin. Drug Discov. 7 (2012) 791–806.
[4] W.A. Lea, A. Simeonov, Fluorescence polarization assays in small molecule screening, Expert Opin. Drug Discov. 6 (2010) 17–32.
[5] K.G. Huwiler, T. De Rosier, B. Hanson, K.W. Vogel, A fluorescence anisotropy assay for the muscarinic M1 G-protein-coupled receptor, Assay Drug Dev. Technol. 8 (2010) 356–366.
[6] A. Harris, S. Cox, D. Burns, C. Norey, Miniaturization of fluorescence polarization receptor-binding assays using CyDye-labeled ligands, J. Biomol. Screen. 8 (2003) 410–420.
[7] P. Cornelius, E. Lee, W. Lin, R. Wang, W. Werner, J.A. Brown, F. Stuhmeier, J.G. Boyd, K. McClure, Design, synthesis, and pharmacology of fluorescently labeled analogs of serotonin: application to screening of the 5-HT2C receptor, J. Biomol. Screen. 14 (2009) 360–370.
[8] E.U. Do, E.B. Jo, G. Choi, L.Z. Piao, J. Shin, M.D. Seo, S.J. Kang, B.J. Lee, K.H. Kim, J.B. Kim, S.I. Kim, Melanocortin 4 receptors interact with antimicrobial frog peptide analogues, Biochem. Biophys. Res. Commun. 343 (2006) 1094–1100.
[9] J.C. Wilkinson, R.A. Stein, C.A. Guyer, J.M. Beechem, J.V. Staros, Real-time kinetics of ligand/cell surface receptor interactions in living cells: binding of epidermal growth factor to the epidermal growth factor receptor, Biochemistry 40 (2001) 10230–10242.

[10] J.W. Jones, T.A. Greene, C.A. Grygon, B.J. Doranz, M.P. Brown, Cell-free assay of G-protein-coupled receptors using fluorescence polarization, J. Biomol. Screen. 13 (2008) 424–429.
[11] S. Veiksina, S. Kopanchuk, A. Rinken, Fluorescence anisotropy assay for pharmacological characterization of ligand binding dynamics to melanocortin 4 receptors, Anal. Biochem. 402 (2010) 32–39.
[12] T.P. Loisel, H. Ansanay, S. St-Onge, B. Gay, P. Boulanger, A.D. Strosberg, S. Marullo, M. Bouvier, Recovery of homogeneous and functional [beta]2-adrenergic receptors from extracellular baculovirus particles, Nat. Biotechnol. 15 (1997) 1300–1304.
[13] A.R. Makela, C. Oker-Blom, The baculovirus display technology—an evolving instrument for molecular screening and drug delivery, Comb. Chem. High Throughput Screen. 11 (2008) 86–98.
[14] V. Janakiraman, W.F. Forrest, B. Chow, S. Seshagiri, A rapid method for estimation of baculovirus titer based on viable cell size, J. Virol. Methods 132 (2006) 48–58.
[15] R.B. Thompson, I. Gryczynski, J. Malicka, Fluorescence polarization standards for high-throughput screening and imaging, Biotechniques 32 (2002) 34–42.
[16] F. Mutulis, S. Yahorava, I. Mutule, A. Yahorau, S. Kopanchuk, S. Veiksina, A. Rinken, J.E.S. Wikberg, A non-peptide radioiodinated high affinity melanocortin-4 receptor ligand, J. Label. Compd. Radiopharm. 46 (2003) 1007–1017.
[17] A. Jablonski, On the notion of emission anisotropy, Bull. Acad. Pol. Sci. Ser. Sci. Math. Astr. Phys. 8 (1960) 259–264.
[18] D.M. Jameson, G. Mocz, Fluorescence polarization/anisotropy approaches to study protein–ligand interactions: effects of errors and uncertainties, Methods Mol. Biol. 305 (2005) 301–322.
[19] O. Nosjean, S. Souchaud, C. Deniau, O. Geneste, N. Cauquil, J.A. Boutin, A simple theoretical model for fluorescence polarization binding assay development, J. Biomol. Screen. 11 (2006) 949–958.
[20] F. Malatesta, The study of bimolecular reactions under non-pseudo-first order conditions, Biophys. Chem. 116 (2005) 251–256.
[21] E.C. Hulme, N.J.M. Birdsall, Strategy and tactics in receptor binding studies, in: E.C. Hulme (Ed.), Receptor–Ligand Interactions. A Practical Approach, IRL Press, Oxford, 1992, pp. 63–176.
[22] M.H. Roehrl, J.Y. Wang, G. Wagner, A general framework for development and data analysis of competitive high-throughput screens for small-molecule inhibitors of protein–protein interactions by fluorescence polarization, Biochemistry 43 (2004) 16056–16066.
[23] Z.X. Wang, An exact mathematical expression for describing competitive binding of two different ligands to a protein molecule, FEBS Lett. 360 (1995) 111–114.
[24] K. Bailey, M. Bally, W. Leifert, J. Voros, T. McMurchie, G-protein coupled receptor array technologies: site directed immobilisation of liposomes containing the H1-histamine or M2-muscarinic receptors, Proteomics 9 (2009) 2052–2063.
[25] K. Masuda, H. Itoh, T. Sakihama, C. Akiyama, K. Takahashi, R. Fukuda, T. Yokomizo, T. Shimizu, T. Kodama, T. Hamakubo, A combinatorial G protein-coupled receptor reconstitution system on budded baculovirus. Evidence for Gai and Gao coupling to a human leukotriene B4 receptor, J. Biol. Chem. 278 (2003) 24552–24562.
[26] O. Mazina, R. Reinart, S. Kopanchuk, A. Rinken, BacMam system for FRET based cAMP sensor expression in studies of melanocortin MC1 receptor activation, J. Biomol. Screen. 17 (2012) 1096–1101.
[27] S. Kopanchuk, S. Veiksina, R. Petrovska, I. Mutule, M. Szardenings, A. Rinken, J.E.S. Wikberg, Co-operative regulation of ligand binding to melanocortin receptor subtypes: evidence for interacting binding sites, Eur. J. Pharmacol. 512 (2005) 85–95.
[28] S. Kopanchuk, S. Veiksina, F. Mutulis, I. Mutule, S. Yahorava, I. Mandrika, R. Petrovska, A. Rinken, J.E.S. Wikberg, Kinetic evidence for tandemly arranged ligand binding sites in melanocortin 4 receptor complexes, Neurochem. Int. 49 (2006) 533–542.
[29] S.A. Nickolls, M.I. Cismowski, X. Wang, M. Wolff, P.J. Conlon, R.A. Maki, Molecular determinants of melanocortin 4 receptor ligand binding and MC4/MC3 receptor selectivity, J. Pharmacol. Exp. Ther. 304 (2003) 1217–1227.
[30] A. Todorovic, C. Haskell-Luevano, A review of melanocortin receptor small molecule ligands, Peptides 26 (2005) 2026–2036.
[31] A. Packeu, M. Wennerberg, A. Balendran, G. Vauquelin, Estimation of the dissociation rate of unlabelled ligand–receptor complexes by a 'two-step' competition binding approach, Br. J. Pharmacol. 161 (2010) 1311–1328.